Chiroptical Properties of 1-Azabicyclo[3.1.0]hexane in the Vacuum-UV and IR Regions

A. Rauk,*,† D. Yang,† D. Tsankov,† H. Wieser,† Yu. Koltypin,‡ A. Gedanken,‡ and G. V. Shustov§

Contribution from the Department of Chemistry, University of Calgary, Calgary, AB, T2N 1N4 Canada, the Department of Chemistry, Bar Ilan University, Ramat Gan 52900, Israel, and the Institute of Chemical Physics, Russian Academy of Sciences, Moscow 117977, Russia

Received November 28, 1994⊗

Abstract: The structure and force field of a bridgehead aziridine, 1-azabicyclo[3.1.0]hexane (ABH), have been determined by ab initio computational methods at three levels, RHF/6-31G*(0.3), MP2/6-31G*, and Becke3LYP/6-31G*. All three methods are shown to give very similar geometries and force fields. The chiroptical properties of ABH have been investigated experimentally and theoretically in the UV region by the ab initio PCI method and in the IR region by the vibronic coupling theory as implemented in the VCT90 program. The UV/CD investigation represents the first such study on an aziridine. The lower electronic transitions of ABH, all of which occur in the vacuum-UV region, are to Rydberg states. No simple chiral rule emerges from the UV/CD study. The experimental vibrational circular dichroism spectrum displays a prominent feature which is due to wagging of the methine hydrogen and obeys a previously identified ||CH methine wagging rule. Comparison of the CEs attributable to local modes of the three-ring methylene group of ABH with analogous published data on related aziridines suggests that some of these modes may serve as indicators of N atom and skeletal absolute configurations.

Introduction

The 1-azabicyclo[3.1.0]hexane skeleton is one of the key fragments of antitumor−antibiotic agents—for example, azinomycins A and B.[1] Hence 1-azabicyclo[3.1.0]hexane (ABH) and similar bicyclic aziridines can be considered as potential precursors of new biologically active compounds. A knowledge of the chiroptical properties of ABH should be a useful basis for stereochemical investigations of such compounds by means of circular dichroism (CD) spectroscopy. From the point of view of structural chemistry, ABH is interesting as a simple model of 1,2-dialkylaziridines in which there is a rigid fastened *cis* orientation of the alkyl groups. The conformation of this compound in solution has been studied by ^{1}H and ^{13}C NMR methods.[2]

Earlier,[3] ABH was obtained in the optically active (1*R*,5*S*)-(−)-form and later[4] an attempt was made to study the chiroptical properties of this compound. However, according to the published CD spectra of (−)-ABH in octane (Figure 4 in ref 4), the maximum of the longest wavelength cotton effect (CE) is outside the accessible region, i.e., below 200 nm. This is not surprising if we consider the high s-character of the nonbonding (n) orbital of the aziridine nitrogen, especially when it is incorporated in a bridgehead of a bicyclic system. It is known that the CE, caused by an electronic transition from the n_N orbital, is observed in the rather short wavelength region (190−205 nm) for even nonstrained amines, e.g., piperidines.[5] Thus, acceptable CD spectra of (1*R*,5*S*)-(−)-ABH can be measured either in the gaseous phase in the vacuum-UV region or in the solution phase in the IR region. In the present work, we have studied both the *electronic* CD (ECD) and *vibrational* CD (VCD) spectra. Nonempirical quantum chemical calculations of ABH have been performed for interpretation of both kinds of CD spectra. As far as we know, hitherto VUV ECD spectra of aziridines have not been previously measured, whereas VCD properties of alkyl-substituted aziridines have been studied in some depth.[6,7]

Results and Discussion

Geometry. Full optimization of the molecular geometry at the RHF level with the 6-31G*(0.3) basis set[8] leads only to the boat form of ABH (Figure 1), as does optimization at Becke3LYP/6-31G* or MP2/6-31G* level. Geometric details are given in Table 1. Each of the three methods yields essentially the same geometry, the largest deviations being of the order of 0.01 Å in bond length and 2° in bond angle. The chair form is not a stationary point on the potential energy surface of topomerization. This result is in agreement with the results of the earlier investigation of ABH by means of NMR spectroscopy.[2] In ref 2 the conclusion about the existence of ABH in the boat form was made on the basis of the upfield shift of the C(3) signal and of the values of the vicinal spin−spin coupling constants of the proton of C(5) with the proton at C(4).

† University of Calgary.
‡ Bar Ilan University.
§ Russian Academy of Sciences.
⊗ Abstract published in *Advance ACS Abstracts*, March 15, 1995.

(1) (a) Moran, E. J.; Tellew, J. E.; Zhao, Z.; Armstrong, R. W. *J. Org. Chem.* **1993**, *58*, 7848−7859. (b) Coleman, R. S.; Carpenter, A. J. *J. Org. Chem.* **1992**, *57*, 5813−5815 and references therein.

(2) Shustov, G. V.; Denisenko, S. N.; Chervin, I. T.; Asfandiarov, N. L.; Kostyanovsky, R. G. *Tetrahedron* **1985**, *41*, 5719−5731.

(3) Gassman, P. G.; Fentiman, A. *J. Org. Chem.* **1967**, *32*, 2388.

(4) Kostyanovsky, R. G.; Gella. I. M.; Markov, V. I., Samojlova, Z. E. *Tetrahedron* **1974**, *30*, 39−45.

(5) Craig, J. C.; Lee, S.-Y. C.; Pereira, W. E., Jr.; Beyerman, H. C.; Maat, L. *Tetrahedron* **1978**, *34*, 501−504.

(6) Rauk, A.; Eggimann, T.; Wieser, H.; Shustov, G. V.; Yang, D. *Can. J. Chem.* **1994**, *72*, 506−513.

(7) Yang, D.; Eggimann, T.; Wieser, H.; Rauk, A.; Shustov, G. *Can. J. Chem.* **1993**, *71*, 2028−2037.

(8) The 6-31G*(0.3) basis set differs from the regular 6-31G* basis set only in that the d orbital exponents have been changed to 0.3 from the default value (0.8). It yields improved geometries and IR and VCD intensities. See: Rauk, A.; Yang, D. *J. Phys. Chem.* **1992**, *96*, 437−446.

0002-7863/95/1517-4160$09.00/0

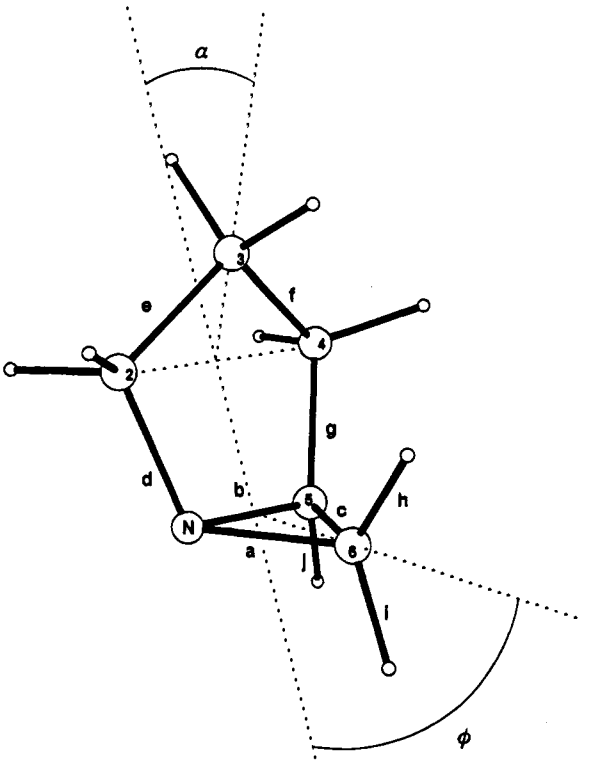

Figure 1. Structure of (1*R*,5*S*)-ABH. Selected structural parameters are listed in Table 1.

Table 1. Optimized Geometry of (1*R*,5*S*)-1-Azabicyclo[3.1.0]hexane

parameter[a]	RHF/6-31G*(0.3) [b]	Becke3LYP/6-31G* [c]	MP2/6-31G* [d]
a	1.475	1.472	1.472
b	1.478	1.480	1.480
c	1.484	1.487	1.481
d	1.477	1.479	1.476
e	1.547	1.549	1.538
f	1.545	1.546	1.535
g	1.522	1.523	1.514
h	1.081	1.090	1.088
i	1.079	1.088	1.086
j	1.080	1.089	1.087
ab	60.4	60.0	60.2
ac	59.9	60.0	60.1
ad	113.9	113.4	112.6
bd	107.2	106.4	105.9
bg	109.5	110.4	110.2
cg	118.2	117.8	117.5
ij	114.7	114.2	114.4
a	25.8	27.1	28.8
ϕ	70.0	70.4	70.9

[a] See Figure 1. *a*, *b*, ... denote bond length in Å; *ab*, *ac*, ... denote bond angles in degrees. [b] $E = -248.91917$ hartree. [c] $E = -250.65559$ hartree. [d] $E = -249.82037$ hartree.

It should be noted that the boat form of ABH is characterized by significant bend angles $a = 70°$ and $\phi = 26°$ (Figure 1)[9] which are similar to the bend angles ($a = 71.4°$, $\phi = 23.8°$) of the molecule of the carbocyclic analog—bicyclo[3.1.0]hexane.[10]

Optical and CD Spectra in the Vacuum-UV Region. The results of the calculation of the relative energies, oscillator strengths, and rotational strengths of the first four electronic transitions of (1*R*,5*S*)-ABH are listed in Table 2. The results were calculated by three methods, PCI with the 6-31+G* basis set, G92 with the same basis set and G92 with the 6-311++G** basis set. The calculated rotatory strengths derived by the three methods are very similar and are in qualitative agreement with the experimental VUV and CD spectra of the compound (Figure 2). Relative to the PCI results, the smaller basis set G92 calculation overemphasizes the negative rotatory strength of the fourth transition, while the larger basis set G92 calculation yields a lower positive value for the rotatory strength of the third transition.

All four of the lowest energy electronic transitions are to singlet states which have much Rydberg character. The lower singly occupied orbital (the originating orbital of the transition) is the same in each case, namely the n_N orbital (Figure 3a) which is the highest occupied molecular orbital (HOMO) for ABH. Each of the lower electronic states may be regarded as the same molecular ion serving as core potential for a "3s" or "3p" electron. The absolute values of the excitation energies are not well represented at the all-singles level of configuration interaction because the theoretical method[11] does not take account of the reorganization of the "unexcited" electrons which accompanies the excitation process. An estimate of the magnitude

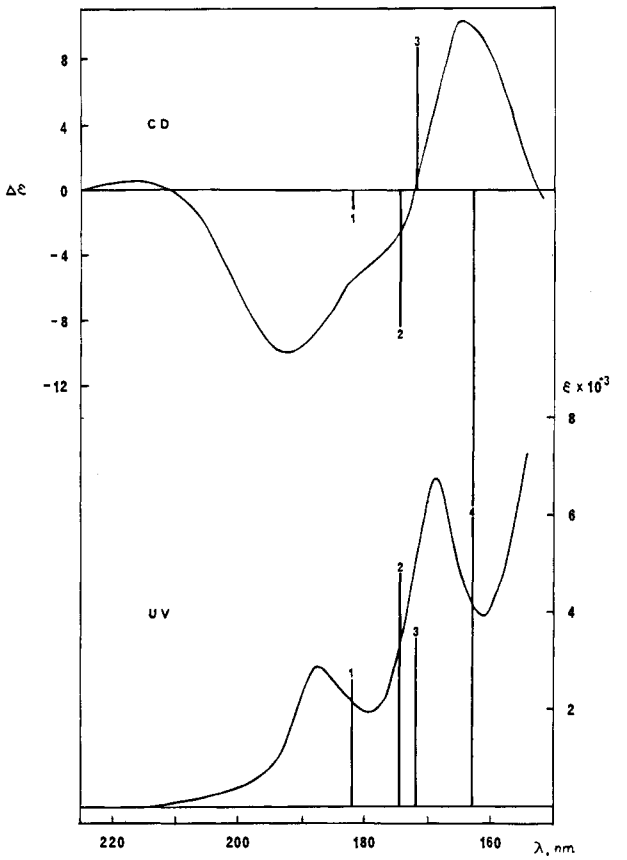

Figure 2. Absorption (—) and CD (– – –) spectra of (1*R*,5*S*)-1-azabicyclo[3.1.0]hexane in the gaseous phase.

Table 2. Electronic States and Transition Properties for (1*R*,5*S*)-1-Azabicyclo[3.1.0]hexane[a]

state	description[b]	ΔE (eV)	ΔE_{cor}[c] (eV)	[R][d] PCI[e]	[R][d] G92[e]	[R][d] G92[f]	*f* PCI[e]	*f* G92[f]
1	n_N-3s	7.83	6.81	−1.1	−1.4	−1.5	0.0078	0.0028
2	n_N-3p	8.12	7.10	−8.3	−5.7	−7.6	0.0144	0.0065
3	n_N-3p	8.24	7.22	+8.7	+9.4	+4.3	0.0103	0.0082
4	n_N-3p	8.63	7.61	−19.4	−26.9	−15.4	0.0179	0.0168

[a] RHF/6-31G*(0.3) geometry (Figure 1, Table 1). [b] See Figure 3. [c] After correction (see text). [d] 10^{-40} cgs. [e] 6-31+G* basis set. [f] 6-311++G** basis set.

(9) The angles α and ϕ (Figure 1) are average values since there is a small twist in the five-membered ring (the dihedral angle dbg is 3.5°).

(10) Mastryukov, V. S.; Osina, E. L.; Vilkov, L. V.; Hilderbrandt, R. L. *J. Am. Chem. Soc.* **1977**, *99*, 6855–6861.

(11) Rauk, A.; Barriel, J. M. *Chem. Phys.* **1977**, *25*, 409–424.

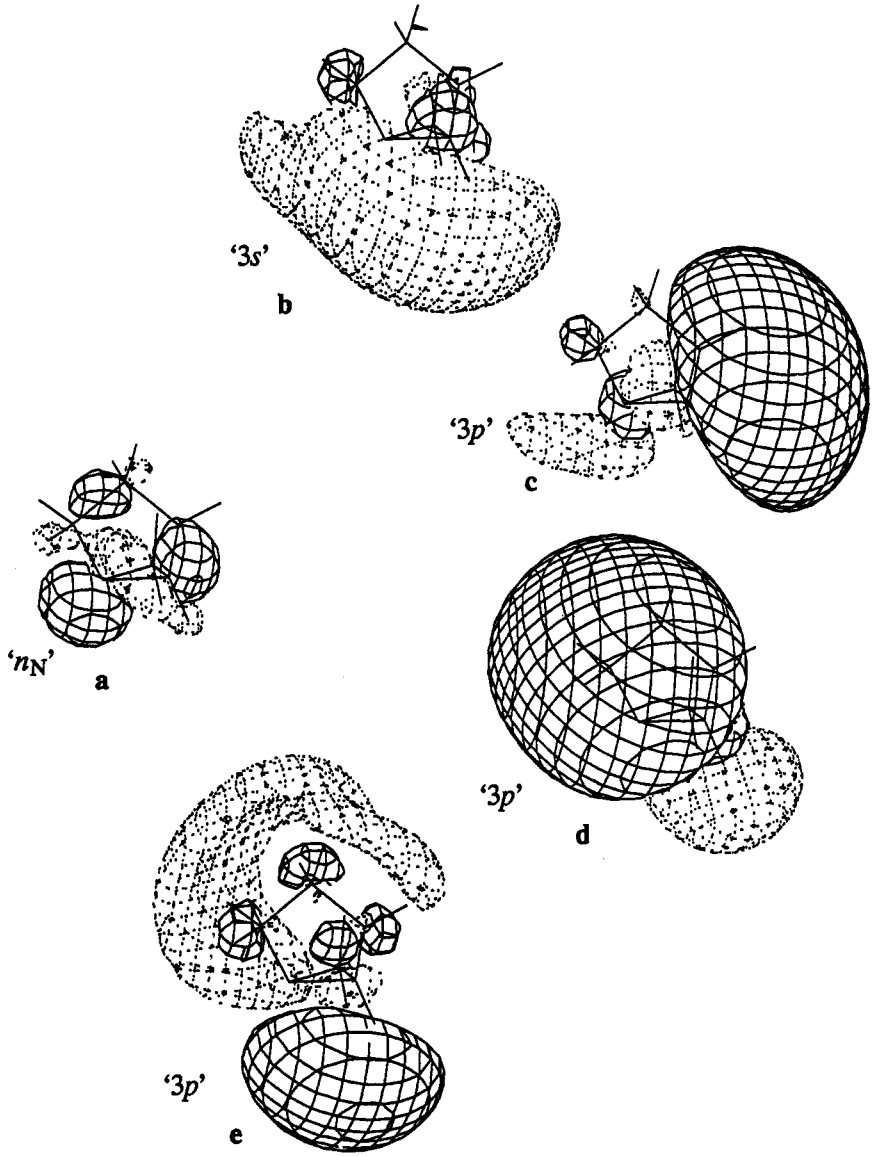

Figure 3. Initial n orbital (MO 23, HOMO) (**a**, contour value 0.05) for all states and the terminal orbitals (**b**–**e**, contour value 0.025) of the lowest excited singlet states of ABH.

of the core molecular ion relaxation energy may be obtained as a correction to Koopmans's theorem for the first ionization potential[12,13] and used for estimation of the error of the transition energies. This correction is found to be 1.02 eV. Subtraction of 1.02 eV from the energy of the first excited state and recalculation of the energies of the rest of the three states with respect to the first one shifts the calculated wavelengths of the transitions into the region 160–190 nm (Table 2) observed experimentally (Figure 2).

If viable sector rules are eventually to be established for aziridines, it is important to understand the nature of the orbitals involved in the electronic transitions. The PCI program permits an analysis of the singly occupied MOs of the excited states by the properties of determinantal wave functions which differ by a single MO.[14] According to the analysis, the initial n_N orbital (Figure 3a) is significantly delocalized by mixing in-phase with one of the Walsh σ orbitals of the aziridine ring and out-of-phase with the σ orbital of the C(2)–C(3) bond, the bond which is approximately anticoplanar to the lone pair on N (bond g, Figure 1). The terminal orbitals of the transitions (i.e., the higher singly occupied orbitals) are hybrids with different contributions of the "3s"- and "3p"-like diffuse orbitals. As one can see from Figure 3b–e, a "3s"-like orbital makes the main contribution in the terminal orbital of the first transition. This orbital may be considered to arise from a linear combination of a 3s orbital of N and the Rydberg conjugate of the valence σ^* orbital[15] of the bond to the methine hydrogen (bond j, Figure 1). The terminal orbitals of the next three transitions can be described as "3p"-like orbitals, oriented in three orthogonal directions. The first two of these are oriented approximately parallel to the plane of the three-membered ring, and the two states are similar in energy. The lower of these sandwiches the five-membered ring, leaving most of the electron density of the larger ring in the region of its nodal surfaces. The third "3p"-like

(12) Pickup, B. T.; Goscinski, O. *Mol. Phys.* **1973**, *26*, 1013–1035: an implementation of eq 38.

(13) The calculated ionization potentials (eV) of ABH according to Koopmans' theorem and after approximate many-body correction (in parentheses) by the method of Pickup and Goscinski (ref 12): MO23, 9.94 (8.92); MO22, 11.73 (10.85); MO21, 12.39 (11.46).

(14) Rauk, A.; Jarvie, J. O.; Ichimura, H.; Barriel, J. M. *J. Am. Chem. Soc.* **1975**, *97*, 5656–5664.

(15) By *Rydberg conjugate of a valence orbital*, we mean the diffuse molecular hydrogen-like orbital which has the same symmetry properties and nodal characteristics as a virtual valence MO. For example, the 3s Rydberg orbital of methane is the Rydberg conjugate of the a_1 combination of the CH σ^* orbitals, and one of the 3d orbitals of ethene is the Rydberg conjugate of the π^* MO.

orbital, corresponding to the fourth excited singlet state, is oriented perpendicular to the three-membered ring and engulfs the five-membered ring. It may be argued that this orbital (and therefore the state) is raised in energy relative to the others by the requirement that it be orthogonal to the greater electron distribution of the larger ring.

From the relative calculated energies of the first four transitions, the first band at 188 nm in the VUV spectrum of ABH (Figure 2) should be assigned to the n_N-3s Rydberg transition and the second band at 169 nm is apparently caused by an overlap of the two lower n_N-3p transitions which are close in energy. The observed intensities ratio for the absorption absorption bands is in the same direction as the calculated value and confirms this assignment.

In the CD spectrum of (1*R*,5*S*)-ABH, the wavelengths of the most intensive CE extrema do not coincide with the wavelengths of the bands in the VUV spectrum (Figure 2). This is an indication that the observed CD spectrum may be the result of a superposition of dichroic absorption bands with different signs. The first negative CE at 193 nm is apparently mainly caused by the n_N-3s transition which is predicted to have a negative rotational strength (Table 2). The short-wavelength shoulder of this CE together with the second positive CE at 165 nm are the result of superposition of the nearly degenerate dichroic bands of the next two n_N-3p transitions, which are predicted to have opposite signs of the rotational strengths. It can be supposed that in fact the second n_N-3p transition has a greater positive rotational strength than is predicted by the calculation and the long-wavelength tail from the dichroic band of this transition gives the small positive extremum at 215 nm. It is difficult to propose another explanation of the appearance of this extremum because the existence of an independent CE (i.e., another electronic transition) in this region is not supported by any of the calculations. The evident negative direction of the CD curve toward the short-wavelength region (below 153 nm) is in agreement with the calculated negative sign of the more intense rotational strength of the fourth n_N-3p transition.

It would be convenient if a reliable sector rule could be devised that relates the CE of a characteristic absorption of aziridines to the absolute configuration. Alkyl-substituted oxiranes are closest to aziridines and, in particular, to ABH in structure and electronic properties and represent the class of three-membered heterocycles for which optical and CD spectra in the vacuum-UV region have been well studied.[16] These compounds have the same origin of the first four electronic transitions[16b,e] as ABH. A quadrant rule,[16c] which connects the CE sign of the n_O-3s transition of the oxirane chromophore with the absolute configuration of chiral carbon centers was proposed. However, the quadrant rule cannot be applied for ABH because, unlike the oxirane chromophore, the aziridine one has lower local symmetry. Besides, in ABH the nitrogen atom, on which the initial and terminal orbitals of the electronic transitions are centered, is a chiral center itself. It may be that the arguments proposed above for the determination of the relative dispositions of the Rydberg 3s and 3p orbitals may help in the development of simpler rules. However, it will require further investigations of alkyl-substituted aziridines before a generalization relating aziridine chirality to electron CD can be developed.

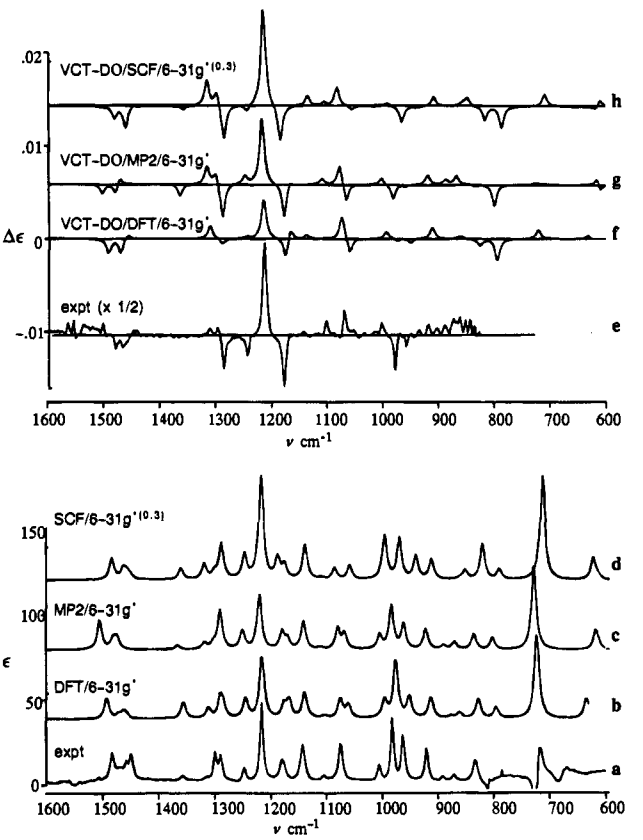

Figure 4. Experimental (**a**, **e**) and theoretical (**b**–**d**, **f**–**h**) IR (**a**–**d**) and VCD (**e**–**h**) spectra (1*R*,5*S*)-1-azabicyclo[3.1.0]hexane: **f**, geometry, force field, and atomic polar tensors at Becke3LYP level; atomic axial tensors at SCF level; **g**, geometry, force field, atomic polar tensors and atomic axial tensors at MP2 level; **h**, geometry, force field, atomic polar tensors and atomic axial tensors at SCF level.

Vibrational Circular Dichroism. Predicted vibrational frequencies and IR and VCD intensities are not tabulated here but are listed in detail in the supplementary material. The results for the IR predictions from each of the methods (RHF/6-31G*$^{(0.3)}$, Becke3LYP/6-31G*, and MP2/6-31G*) are qualitatively very similar. The experimental IR and VCD spectra in the region 800–1500 cm^{-1} are displayed in Figure 4 and compared with simulations based on the theoretical predictions of all three methods. For the purpose of the simulations, the calculated frequencies have been scaled by standard factors to compensate for systematic overestimation (0.9 for RHF, 0.95 for MP2). The MP2 scale factor was applied to the Becke3LYP values as well. The bands were assumed to be Lorentzian with peak half-width at half-height of 5 cm^{-1}.

A detailed analysis of the IR and VCD spectra of ABH is beyond the scope of the present paper. All of the primary computational data are included in the supplementary material.

We present here an analysis of the principal features of the IR and VCD spectra and relate the ABH results to the results of VCD studies on other aziridine systems, focusing primarily on the chiroptical properties. It is immediately apparent from inspection of Figure 4 that the principal features of both the experimental IR and VCD spectra (Figures 4a and 4e, respectively) are very well reproduced by all of the variations of the ab initio procedures. The most obvious differences are seen: (a) near 1300 cm^{-1}, where the intensity of the high-frequency side of the observed resolved doublet is predicted to be too low

(16) (a) Levi, M.; Arad-Yellin, R.; Green, B. S.; Gedanken, A. *J. Chem. Soc., Chem. Commun.* **1980**, 847. (b) Cohen, D.; Levi, M.; Basch, H.; Gedanken, A. *J. Am. Chem. Soc.* **1983**, *105*, 1738–1742. (c) Gedanken, A.; Hintzer, K.; Schurig, V. *J. Chem. Soc., Chem. Commun.* **1984**, 1615–1616. (d) Gedanken, A.; Schurig, V. *J. Phys. Chem.* **1987**, *91*, 1324–1327. (e) Carnell, M.; Peyerimhoff, S. D.; Breest, A.; Godderz, K. H.; Ochmann, P.; Hormes, J. *Chem. Phys. Lett.* **1991**, *180*, 477–481. (f) Basil, A.; Ben-Tzur, S.; Gedanken, A.; Rodger, A. *Chem. Phys. Lett.* **1991**, *180*, 482–484. (g) Ben-Tzur, S.; Basil, A.; Gedanken, A.; Moore, J. A.; Schwab, J. M. *J. Am. Chem. Soc.* **1992**, *114*, 5751–5753.

Table 3. Comparison of the Predicted Chiroptical Features due to the Methylene Group of (1*R*,5*S*)-Azabicyclo[3.1.0]hexane (ABH), (2*S*)-2-Methylaziridine (MA), and (1*S*,2*S*)-1,2-Dimethylaziridine (DMA)

	(1*R*,5*S*)-ABH			*cis*-(1*R*,2*S*)-MA[a]			*trans*-(1*S*,2*S*)-MA[a]			(1*S*,2*S*)-DMA[b]		
motion	mode	[R][c]	freq[d]	mode	[R][c]	freq[d]	mode	[R][c]	freq[d]	mode	[R][c]	freq[d]
twist	ν_{13}	−5.8	984	ν_6	−6.2	891	ν_6	+2.3	871	ν_9	+14.0	874
	ν_{14}	+2.6	1005	ν_7	+4.1	926	ν_7	−20.4	929	ν_{11}	+4.3	1000
wag	ν_{15}	−6.8	1068	ν_{10}	−1.2	1080	ν_{10}	+18.0	1069	ν_{13}	+4.2	1076
	ν_{16}	+7.3	1080	ν_{11}	+0.6	1114	ν_{11}	+9.1	1096	ν_{14}	+2.8	1090
rock	ν_{18}	−0.3	1142	ν_{14}	+12.0	1237	ν_{14}	+8.6	1243	ν_{17}	−1.3	1173
				ν_{15}	+9.6	1268	ν_{15}	−21.9	1250			
scissor	ν_{29}	−2.7	1482	ν_{17}	−9.0	1400	ν_{17}	−0.2	1412	ν_{22}	−4.0	1400
	ν_{30}	−2.3	1506	ν_{20}	−2.8	1481	ν_{20}	+2.8	1496	ν_{27}	+6.4	1469

[a] Reference 6. [b] Reference 7. [c] cgs × 10^{-44}. [d] cm^{-1}.

Scheme 1. Chiral Rule for ||CH Mode

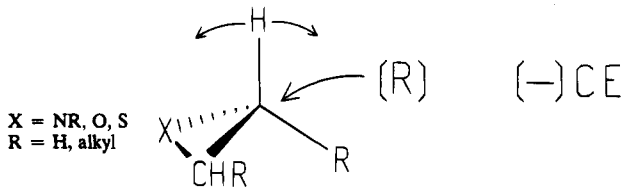

by all three methods, (b) near 1180 and 1080 cm^{-1}, where the experimental IR spectrum exhibits a single (unresolved) band that is predicted to be split into two by all three methods, and (c) between 900 and 1000 cm^{-1} where the predicted relative intensities of the four peaks are at variance with the observed intensities, the MP2/6-31G* method yielding the closest match to the experimental observations.

The experimental VCD spectrum contains a distinctive grouping of CEs in the region 1150−1300 cm^{-1}. These features are reproduced quite well by the three theoretical methods, yielding a definitive assignment of the absolute configuration. Indeed, the single most obvious discrepancy between the observed VCD spectrum and the theoretical predictions occurs for the weak CE at 1240 cm^{-1}, for which only the VCT-DO/SCF/6-31G*$^{(0.3)}$ procedure yields the correct sign.

The most prominent feature of the experimental VCD spectrum, the positive CE at 1210 cm^{-1} also coincides with the most intense IR absorption in this vicinity. This feature is assigned to wagging of the methine bond in the plane of bonds g and j (Figure 1) mixed with twisting motions of the methylene groups at C(2) and C(4). A chiral rule associated with this "parallel" motion of the methine hydrogen has previously been identified and shown to hold in simple aziridines, oxiranes, and thiiranes.[7] The rule is displayed in Scheme 1. In each case where the ||CH mode could be identified in the VCD spectrum, the motion in a local environment of (*R*) chirality is associated with a negative CE, and vice versa (the present case).

The second most prominent feature in the experimental VCD spectrum is the adjacent negative CE at 1185 cm^{-1}, which is assigned to wagging motions of the equatorial C−H bonds at C(2), C(3), and C(4), with the largest amplitude motion at C(4). The large value of the CE is not due to especially large magnitudes of the electric dipole transition moment or the magnetic dipole transition moment but rather to the significant deviation from an orthogonal orientation of the two vectors (the angle between the MP2/6-31G* magnetic and electric dipole transition moment vectors is 119°). The vibrational motion responsible for this feature is largely localized to the five-membered ring and would not be associated with the aziridine functionality in general.

It is illuminating to look for similarities in the measured and theoretically predicted VCD spectra of *cis*-2-methylaziridine ((1*R*,2*S*)-MA),[6] *trans*-2-methylaziridine ((1*S*,2*S*)-MA),[6] and 1,2-dimethylaziridine ((1*S*,2*S*)-DMA).[7] All three compounds and ABH have one methine proton adjacent to the nitrogen, and all follow the ||CH methine rule mentioned above. Another common feature of the three simpler aziridines and ABH is the presence of the methylene group in the three-membered ring. Examination of the twisting, wagging, rocking, and scissoring motions expected of the methylene group reveals some features which may indicate correlation with the absolute configuration at N or with the chirality of the skeleton defined by the σ bonds. The analysis is somewhat complicated by the fact that each of the local group motions is mixed with other vibrational motions and so appears in more than one normal mode. The data are summarized in Table 3. The signs of CEs mentioned in the following discussion and in Table 3 are corrected for the same configuration, *S*, at the asymmetric carbon atom of each of the compounds. In ABH, the CH_2 twist contributes significantly

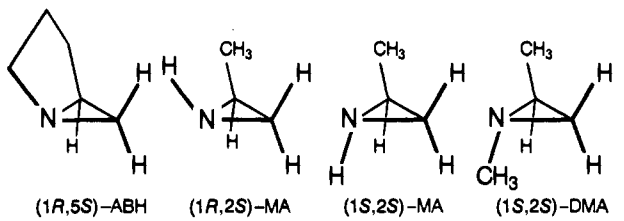

to ν_{13} and ν_{14} at 984 and 1005 cm^{-1}, with predicted and observed (Figure 4) negative and positive CEs, respectively. Exactly the same 2-fold mixing of the twisting mode and the same pattern of signs is predicted for *cis*-2-methylaziridine ((1*S*,2*S*)-MA), which most closely models ABH. The lower frequency mode reverses in sign with reversal of the absolute configuration at N. The second does also in ((1*S*,2*S*)-MA) but not in ((1*S*,2*S*)-DMA). The CH_2 wag also contributes to at least two vibrational modes in each compound (Table 3). The first of these reverses sign with reversal of the configuration at N but the second does not, being predicted and observed to have a positive CE in each compound. No clear pattern emerges from inspection of the involvement of the rocking mode, which is predicted to dominate one normal mode of ABH (ν_{18}) but to have very small rotatory strength. The CH_2 scissor also contributes to at least two modes in each compound. The lower frequency combination is predicted to have a negative CE in each case, while the higher changes sign with configuration at N. The present set of compounds suggests the possibility of identifying local modes which may serve as chiral indicators. However, the sample size is too small. Further investigations on related compounds are required to determine whether the correlations discussed above are general.

Methods

Experimental Section. (1*R*,5*S*)-1-Azabicyclo[3.1.0]hexane ((1*R*,5*S*)-ABH), bp 105−106 °C, $[\alpha]^{20}_D$ −23.9° (*c* 2.9, heptane) was obtained

from (*S*)-(+)-2-pyrrolidinemethanol (Aldrich) according to ref 3 and shows satisfactory spectral data.

The vacuum-UV CD instrument used in this study has been described previously. The monochromator used for the measurements is a McPherson 225 equipped with a 1200 lines/mm grating yielding a spectral resolution of 8 Å/mm. All the CD and absorption measurements were carried out with a 2 mm slit width. The sample was introduced into a 10 cm path length cell after a few freeze−pump−thaw cycles. The vapor pressure was measured by a Wallace and Tiernan absolute pressure gauge.

The VCD spectra were measured in the range 800−1600 cm^{-1} at 4 cm^{-1} resolution on the University of Calgary VCD instrument described in detail elsewhere.[17] The spectra were recorded at CCl_4 solutions. Extreme care was taken to keep the solution dry and prevent possible polymerization of the sample. The CCl_4 solvent was freshly distilled over P_2O_5 and kept over molecular sieves in a sealed flask. The infrared liquid cell was assembled with a new pair of NaCl windows and a 0.15 mm lead spacer. The syringe used to fill the cell was dried for some hours in an oven. The data acquisition was done in real time, and the spectrum was monitored after every 100 scans. The first signs of the onset of polymerization were noticed after the first 10 min when 500 ac scans were collected. The ac block was ratioed with 50 dc scans obtained immediately after the ac collection. The base-line artifacts were removed by subtraction of the solvent "VCD" spectrum.

Computational Section. The structure of ABH was fully optimized at the Hartree−Fock (RHF) level with a modified 6-31G* basis set designated as 6-31G*$^{(0.3)}$, and at second-order Moller−Plesset (MP2) and density functional theoretical levels, both with the internal 6-31G* basis set, using procedures implemented in the Gaussian 92/DFT system of programs.[18] In the case of the MP2 calculations, all of the orbitals were used.

For the DFT calculations, a hybrid approach based on Becke's three-parameter functional[19] was employed (Becke3LYP). The functional form is

$$(1 - a_0)E_X^{LSDA} + a_0E_X^{HF} + a_X\Delta E_X^{B88} + a_CE_C^{LYP} + (1 - a_C)E_C^{VWN}$$

where the energy terms are the Slater exchange, the Hartree−Fock exchange, Becke's 1988 exchange functional correction,[20] the gradient correlation functional of Lee, Yang, and Parr,[21] and the local correlation functional of Vosko, Wilk, and Nusair,[22] respectively. The values of the coefficients determined by Becke are

$$a_0 = 0.20, \quad a_X = 0.72, \quad a_C = 0.81$$

At each level, a boatlike conformation (Figure 1) was found. Attempts to locate a chairlike conformation at the RHF/6-31G*$^{(0.3)}$ and Becke3LYP/6-31G* levels resulted in conversion to the boat-like form.

Harmonic vibrational analysis was carried out at each level. For the purpose of comparing frequencies with experimental values, the RHF frequencies were scaled uniformly by 0.9 and the MP2/6-31G* and Becke3LYP/6-31G* values were similarly scaled by 0.95.

Chiroptical properties in the VUV region were calculated using the PCl and Gaussian 92 programs and the 6-31+G* basis set at the RHF/6-31G*$^{(0.3)}$ geometry. The use of the diffuse s and p functions designated by the "+" is desirable for a more accurate description of the diffuse excited singlet states. The PCl program determines optical rotatory strengths and dipole oscillator strengths from electric and magnetic dipole transition moments which are correct to first order in Rayleigh−Schrödinger perturbation theory. Both the ground state and excited states are partitioned into zero (strongly interacting) and first-order (weakly interacting) contributions. Only single excitation CI is carried out for the excited states over a window limited to 15 occupied and 50 unoccupied orbitals. Electron correlation of the ground state wave function is taken into account in the form of doubly excited configurations derived from the same window as first-order corrections to the zero-order Hartree-Fock single determinantal wave function. PCl has been extensively used,[23] and the theory is described in detail elsewhere.[11] Electronic chiroptical properties may also be obtained from Gaussian 92 by specifying CIS. An all-singles CI calculation is carried out for a specified number of electronic states, and values of electric and magnetic dipole transition moments are calculated. The magnetic dipole transition moments are for a ground state to excited state transition and must be reversed in sign when used to calculate rotatory strengths. The results correspond to PCl values prior to addition of the ground state correlation term. However, Gaussian 92 permits the use of a much larger basis set than does PCl in its current implementation. Results using the 6-311++G** basis set are also reported.

Molecular orbitals are displayed as modified Jorgensen−Salem plots.[24]

Chiroptical properties in the IR region are calculated using the VCT90 computer code,[25,26] which implements the vibronic coupling theory of vibrational circular dichroism intensities derived by Nafie and Freedman.[27] Accurate *a priori* prediction of VCD intensities requires geometry optimization and harmonic frequency analysis prior to the evaluation of electric and magnetic dipole transition moments. The magnetic quantities are gauge origin dependent. We report here results calculated in the distributed origins (DO) with origins at nuclei gauge proposed by Stephens[28] and incorporated into VCT.[29] Extensive experience with the prediction of VCD intensities has confirmed that the single most important factor for semiquantitative results, once a reasonable basis set is chosen, is the quality of the force field as reflected by the cartesian displacement vectors which describe the normal modes. The 6-31G*$^{(0.3)}$ basis set which was originally developed to reproduce VCD intensities produced from a much larger basis set VCT calculation[8] usually yields SCF geometries and force fields comparable in quality to MP2/6-31G* geometries and force fields. The latter are extremely tedious to obtain for larger systems but may be required for molecules with unusual bonding. Accordingly, the geometry and force field of ABH were derived at this level and the VCD intensities predicted with inclusion of ground state electron correlation up to the MP2 level.[30] Density functional-based methods also yield results superior to HF results in most cases, with little extra expenditure of resources. We have also used a hybrid HF−DFT approach as implemented in Gaussian 92 and described above to derive the geometry, force field, and electric dipole transition moments. As magnetic dipole transition moments are not available with this theoretical model, we have substituted the corresponding SCF/6-31G*$^{(0.3)}$-derived quantities.

Conclusions

The chiroptical properties of a bridgehead aziridine, 1-azabicyclo[3.1.0]hexane (ABH), have been investigated experimentally and theoretically in both the UV and IR regions of the spectrum. The UV/CD investigation represents the first such

(17) Tsankov, D.; Eggimann, T.; Wieser, H. *Appl. Spectrosc.* Submitted for publication.

(18) Frisch, M. J.; Trucks, G. W.; Head-Gordon, M.; Gill, P. M. W.; Wong, M. W.; Foresman, J. B.; Johnson, B. G.; Schlegel, H. B.; Robb, M. A.; Replogle, E. S.; Gomperts, R.; Andres, J. L.; Raghavachari, K.; Binkley, J. S.; Gonzalez, C.; Martin, R. L.; Fox, D. J.; Defrees, D. J.; Baker, J.; Stewart, J. J. P.; Pople, J. A. *Gaussian 92, Revision B*; Gaussian, Inc.: Pittsburgh, PA, 1992.

(19) Becke, A. D. *J. Chem. Phys.* **1993**, *98*, 5648.

(20) Becke, A. D. *Phys. Rev. A.* **1988**, *38*, 3098.

(21) Lee, C.; Yang, W.; Parr, R. G. *Phys. Rev. B* **1988**, *37*, 785.

(22) Vosko, S. H.; Wilk, L. Nusair, M. *Can. J. Phys.* **1980**, *58*, 1200.

(23) (a) Shustov, G. V.; Varlamov, S. V.; Rauk, A.; Kostyanovsky, R. G. *J. Am. Chem. Soc.* **1990**, *112*, 3403−3408. (b) Shustov, G. V.; Kadorkina, G. K.; Varlamov, S. V.; Kachanov, A. V.; Kostyanovsky, R. G.; Rauk, A. *J. Am. Chem. Soc.* **1992**, *114*, 1616−1623. (c) Shustov, G. V.; Kadorkina, G. K.; Kostyanovsky, R. G.; Rauk, A. *J. Am. Chem. Soc.* **1988**, *110*, 1719−1726. (d) Shustov, G. V.; Kachanov, A. V.; Kadorkina, G. K. Kostyanovsky, R. G.; Rauk, A. *J. Chem. Soc., Chem. Commun.* **1992**, 705−706. (e) Shustov, G. V.; Kachanov, A. V.; Kadorkina, G. K.; Kostyanovsky, R. G.; Rauk, A. *J. Am. Chem. Soc.* **1992**, *114*, 8257−8262. (f) Shustov, G. V.; Varlamov, S. V.; Rauk, A.; Kostyanovsky, R. G. *J. Am. Chem. Soc.* **1990**, *112*, 3403.

(24) Jorgensen, W. L.; Salem, L. *The Organic Chemists Book of Orbitals*; Academic Press: New York, 1973.

(25) Yang, D.; Rauk, A. *J. Chem. Phys.* **1992**, *97*, 6517.

(26) Yang, D. Ph.D. dissertation, The University of Calgary, 1992.

(27) Nafie, L. A.; Freedman, T. B. *J. Chem. Phys.* **1983**, *78*, 7108.

(28) Stephens, P. J. *J. Phys. Chem.* **1987**, *91*, 1712.

(29) Rauk, A. *J. Am. Chem. Soc.* **1984**, *106*, 6517−6524.

(30) Yang, D.; Rauk, A. *J. Chem. Phys.* **1994**, *100*, 7995−8002.

study on an aziridine. The lower electronic transitions, all of which occur in the vacuum UV region, are shown to terminate in Rydberg states which may be loosely categorized as n_N-3s, and n_N-3p (three states). No simple chiral rule emerges from the UV/CD study. On the other hand, the principle feature of the VCD spectrum is shown to obey a previously identified ||CH methine wagging rule. Comparison of the CEs attributable to local modes of the three-ring methylene group of ABH with analogous published data on related aziridines suggests that some of these modes may serve as indicators of N atom and skeletal absolute configurations.

Acknowledgment. We gratefully thank the Natural Sciences and Engineering Council of Canada for financial support of this work. Partial support is also provided by NATO in the form of a NATO Linkage Grant.

Supplementary Material Available: Tables of optimized geometries, frequencies, dipole and rotatory strengths, illustrations of normal modes, frequencies, and rotatory and oscillator strengths of (1R,5S)-1-azabicyclo[3.1.0]hexane (9 pages). This material is contained in many libraries on microfiche, immediately follows this article in the microfilm version of the journal, can be ordered from the ACS, and can be downloaded from the Internet; see any current masthead page for ordering information and Internet access instructions.

JA943839L